Fermilab FERMILAB-Pub-02/059-E April 2002

New measurements of the D^0 and D^+ lifetimes

The FOCUS Collaboration*

J. M. Link [a], M. Reyes [a], P. M. Yager [a], J. C. Anjos [b], I. Bediaga [b], C. Göbel [b], J. Magnin [b], A. Massafferri [b], J. M. de Miranda [b], I. M. Pepe [b], A. C. dos Reis [b], S. Carrillo [c], E. Casimiro [c], E. Cuautle [c], A. Sánchez-Hernández [c], C. Uribe [c], F. Vázquez [c], L. Agostino [d], L. Cinquini [d], J. P. Cumalat [d], B. O'Reilly [d], J. E. Ramirez [d], I. Segoni [d], J. N. Butler [e], H. W. K. Cheung [e], G. Chiodini [e], I. Gaines [e], P. H. Garbincius [e], L. A. Garren [e], E. Gottschalk [e], P. H. Kasper [e], A. E. Kreymer [e], R. Kutschke [e], L. Benussi [f], S. Bianco [f], F. L. Fabbri [f], A. Zallo [f], C. Cawlfield [g], D. Y. Kim [g], A. Rahimi [g], J. Wiss [g], R. Gardner [h], A. Kryemadhi [h], Y. S. Chung [i], J. S. Kang [i], B. R. Ko [i], J. W. Kwak [i], K. B. Lee [i], K. Cho [j], H. Park [j], G. Alimonti [k], S. Barberis [k], M. Boschini [k], P. D'Angelo [k], M. DiCorato [k], P. Dini [k], L. Edera [k], S. Erba [k], M. Giammarchi [k], P. Inzani [k], F. Leveraro [k], S. Malvezzi [k], D. Menasce [k], M. Mezzadri [k], L. Milazzo [k], L. Moroni [k], D. Pedrini [k], C. Pontoglio [k], F. Prelz [k], M. Rovere [k], S. Sala [k], T. F. Davenport III [ℓ], V. Arena [m], G. Boca [m], G. Bonomi [m], G. Gianini [m], G. Liguori [m], M. M. Merlo [m], D. Pantea [m], S. P. Ratti [m], C. Riccardi [m], P. Vitulo [m], H. Hernandez [n], A. M. Lopez [n], H. Mendez [n], L. Mendez [n], E. Montiel [n], D. Olaya [n], A. Paris [n], J. Quinones [n], C. Rivera [n], W. Xiong [n], Y. Zhang [n], J. R. Wilson [o], T. Handler [p], R. Mitchell [p], D. Engh [q], M. Hosack [q], W. E. Johns [q], M. Nehring [q], P. D. Sheldon [q], K. Stenson [q], E. W. Vaandering [q], M. Webster [q], M. Sheaff [r]

[a] *University of California, Davis, CA 95616*

[b] *Centro Brasileiro de Pesquisas Físicas, Rio de Janeiro, RJ, Brasil*

[c] *CINVESTAV, 07000 México City, DF, Mexico*

[d] *University of Colorado, Boulder, CO 80309*

[e] *Fermi National Accelerator Laboratory, Batavia, IL 60510*
[f] *Laboratori Nazionali di Frascati dell'INFN, Frascati, Italy I-00044*
[g] *University of Illinois, Urbana-Champaign, IL 61801*
[h] *Indiana University, Bloomington, IN 47405*
[i] *Korea University, Seoul, Korea 136-701*
[j] *Kyungpook National University, Taegu, Korea 702-701*
[k] *INFN and University of Milano, Milano, Italy*
[ℓ] *University of North Carolina, Asheville, NC 28804*
[m] *Dipartimento di Fisica Nucleare e Teorica and INFN, Pavia, Italy*
[n] *University of Puerto Rico, Mayaguez, PR 00681*
[o] *University of South Carolina, Columbia, SC 29208*
[p] *University of Tennessee, Knoxville, TN 37996*
[q] *Vanderbilt University, Nashville, TN 37235*
[r] *University of Wisconsin, Madison, WI 53706*

Abstract

A high statistics sample of photoproduced charm particles from the FOCUS (E831) experiment at Fermilab has been used to measure the D^0 and D^+ lifetimes. Using about 210 000 D^0 and 110 000 D^+ events we obtained the following values: 409.6 ± 1.1 (statistical) ± 1.5 (systematic) fs for D^0 and 1039.4 ± 4.3 (statistical) ± 7.0 (systematic) fs for D^+.

The study of the charm hadron lifetimes has been fundamental for our understanding of the heavy quark decays. The most important contribution is the spectator diagram which contributes equally to the widths of all hadrons of a given flavour [1]. In the early days of charm physics it was quite a surprize when the experiments measured a large value for τ_{D^+}/τ_{D^0}. It is generally believed that this large ratio (~ 2.5) is mainly due to the destructive interferences between different quark diagrams that contribute only to D^+ decays. The increasingly precise measurements of the heavy quark lifetimes have stimulated the development of theoretical models, like the Heavy Quark Theory [2], which are able to predict a successful description of the rich pattern in the weak lifetimes of charm hadrons. This is interesting in light of the fact that the charm lifetimes differ by an order of magnitude between the longest (D^+) and the shortest (Ω_c^0) lived.

In this letter we present the most accurate measurement to date of the life-

⋆ See http://www-focus.fnal.gov/authors.html for additional author information.

times of the D^+ and D^0. The accuracy reached by the previous experiments is remarkable, for example the D^0 lifetime is known with an uncertainty of $\sim 1\%$ [3]. However, an important test to validate the measurement of lifetime difference in the neutral D-meson system (in order to determine the parameter $y = \Delta\Gamma/2\Gamma$ of the $D^0 - \overline{D}^0$ mixing [4]) is that the measured D^0 lifetime be consistent with the world average. Therefore the most precise determination of the D^0 lifetime is needed.

Charmed particles were produced by the interaction of high energy photons, obtained by means of bremsstrahlung of electron and positron beams (with typically 300 GeV endpoint energy), with a beryllium oxide target. The mean energy of the photon beam was approximately 180 GeV. The data were collected at Fermilab during the 1996–97 fixed-target run. More than 6.3×10^9 triggers were collected from which more than 1 million charmed particles have been reconstructed.

The particles from the interaction are detected in a large-aperture magnetic spectrometer with excellent vertex measurement, particle identification and calorimetric capabilities. The vertex detector consists of two systems of silicon microvertex detectors. The upstream system consists of 4 planes interleaved with the experimental target, while the downstream system consists of 12 planes of microstrips arranged in three views. These detectors provide high resolution separation of primary (production) and secondary (decay) vertices with an average proper time resolution of $\sim$ 35 fs. The momentum of the charged particles is determined by measuring their deflections in two analysis magnets of opposite polarity with five stations of multiwire proportional chambers. Kaons and pions in the D-meson final states are well separated up to 60 GeV/c of momentum using three multicell threshold Čerenkov counters.

The final states are selected using a candidate driven vertex algorithm [5]. A secondary vertex is formed from the reconstructed tracks and the momentum vector of the D candidate is used as a *seed* to intersect the other tracks in the event to find the primary vertex. Once the production and decay vertices are determined, the distance ℓ between them and the relative error σ_ℓ are computed. Cuts on the ℓ/σ_ℓ ratio are applied to extract the D signals from the prompt background. The primary and secondary vertex are required to have a confidence level greater than 1%.

The vertices (primary and secondary) have to lie inside a *fiducial volume*[1] and the primary vertex must be formed with at least two reconstructed tracks in addition to the *seed* track. The Čerenkov particle identification cuts used

[1] The reason for this cut is the presence of a trigger counter just upstream of the second microstrip device, therefore we define the *fiducial volume* as the region between the first slab of the experimental target and this trigger counter.

in FOCUS are based on likelihood ratios between the various stable particle identification hypotheses. These likelihoods are computed for a given track from the observed firing response (on or off) of all cells within the track's ($\beta = 1$) Čerenkov cone for each of our three Čerenkov counters. The product of all firing probabilities for all cells within the three Čerenkov cones produces a χ^2-like variable $W_i = -2\ln(\text{Likelihood})$ where i ranges over the electron, pion, kaon and proton hypotheses (see reference [6] for more details). We require $\Delta_K \equiv W_\pi - W_K > 1$, called *kaonicity*, for the tracks reconstructed as a kaon. Analogously the tracks reconstructed as pions have a *pionicity*, $\Delta_\pi \equiv W_K - W_\pi$, exceeding 1.

In Figure 1a and 1b we show the invariant mass plots obtained with this set of cuts and with $\ell/\sigma_\ell > 9$ for the decay modes $D^0 \to K^-\pi^+$ and $D^0 \to K^-\pi^+\pi^+\pi^-$ respectively (throughout this paper the charge conjugate state is implied). Figure 1c is the invariant mass plot for the decay mode $D^+ \to K^-\pi^+\pi^+$ with $\ell/\sigma_\ell > 14$. This set of cuts is chosen to optimize the yield and the background underneath the signal (S/N ratio).

From a binned maximum likelihood fit we find $139\,433 \pm 520$ $D^0 \to K^-\pi^+$, $68\,274 \pm 360$ $D^0 \to K^-\pi^+\pi^+\pi^-$ and $109\,877 \pm 385$ $D^+ \to K^-\pi^+\pi^+$ candidates. The plots are fit with two Gaussians with the same mean but different widths to take into account the different resolution in momentum of the tracks passing through one or two magnets (see reference [5] for more details) of our spectrometer plus a 2^{nd} order polynomial. The low mass region is excluded in the fit to avoid possible contamination due to other hadronic charm decays involving an additional π^0.

The lifetime is measured using a binned maximum likelihood fitting technique [7]. A fit is made to the reduced proper time distribution in the signal region. The reduced proper time is defined by $t' = (\ell - N\sigma_\ell)/(\beta\gamma c)$ where ℓ is the distance between the primary and the secondary vertex, σ_ℓ is the resolution on ℓ and N is the minimum "detachment" cut required to extract the signal. Our vertexing algorithm provides very uniform reduced proper time acceptance even at very low reduced proper times. If absorption and acceptance corrections are small enough that they can be neglected, and if σ_ℓ is independent of ℓ, one can show that the t' distribution for decaying charmed particles will follow an exponential distribution. These assumptions are very nearly true in FOCUS [5].

The signal region reduced proper time distributions (indicated with dashed lines in Fig.1) are formed from events with invariant mass within $\pm 2\overline{\sigma}$ of the mean D mass; $\overline{\sigma}$ stands for weighted sigma because the invariant mass plots were fitted with two Gaussians. The dependence of the lifetime measurement on the choice of the signal and background region is discussed later in the text. The binned maximum likelihood method allows direct use of the proper time

distribution of the data above and below the D mass peak to represent the background underneath the signal instead of using a background parametrization. We have chosen two sidebands starting $4\overline{\sigma}$ above and below the mean D mass, each half as wide as the signal region (indicated with dotted lines in Fig.1). The signal and background reduced proper time distributions are binned in proper time wide bins (200 fs) spanning about 10 nominal lifetimes.

The observed numbers of events in a reduced proper time bin i (centered at t'_i) in the signal and sideband histograms are labeled s_i and b_i respectively. The predicted number of events n_i in a reduced proper time bin is given by:

$$n_i = (N_s - B)\frac{f(t'_i)\exp(-t'_i/\tau)}{\sum_i f(t'_i)\exp(-t'_i/\tau)} + B\frac{b_i}{\sum b_i} \tag{1}$$

where N_s is the total number of events in the signal region, B is the total number of background events in the signal region and $f(t'_i)$ is a correction function. The fit parameters are B and τ. The $f(t'_i)$ correction function, derived from a Monte Carlo simulation, corrects the reduced proper time evolution of the signal for the effects of geometric acceptance, reconstruction efficiency, analysis cuts, hadronic absorption and decay of charm secondaries. The use of a multiplicative $f(t'_i)$ correction, rather than an integral over a resolution factor, is justified since our reduced proper time resolution (~ 35 fs) is much less than the D^0 or D^+ lifetime.

A separate $f(t')$ correction function is used for each of the three decay modes. Our Monte Carlo simulation includes the Pythia [8] model for photon-gluon fusion and incorporates a complete simulation at the digitization level of all detector and trigger systems and includes all known multiple scattering and particle absorption effects. The Monte Carlo was run with $\sim$ 15 times the statistics of the experiment.

The plots a) of Figure 2, 3 and 4 show the correction function $f(t')$ for the three decay modes in bins of reduced proper time. The $f(t')$ function is obtained by dividing the simulated reconstructed charm yield in each bin by the input decay exponential. The fall off in $f(t')$ for the D^+ case is due to the exclusion of long lived events with vertices downstream of the fiducial volume[1].

A factor $\mathcal{L}_{\rm bg}$ is included in the likelihood function in order to relate B to the number of background events expected from the side band population. The background level is thereby jointly determined from the invariant mass distribution and from the reduced proper time evolution in the side bands. The likelihood function is then given by:

$$\mathcal{L} = \mathcal{L}_{\rm signal} \times \mathcal{L}_{\rm bg} \tag{2}$$

where

$$\mathcal{L}_{\rm signal} = \prod_{i=1}^{\rm bins} \frac{n_i^{s_i}\,\exp(-n_i)}{s_i!} \tag{3}$$

and

$$\mathcal{L}_{\rm bg} = \frac{B^{N_{\rm bg}}}{N_{\rm bg}!}\exp(-B) \tag{4}$$

with $N_{\rm bg} = \sum_i b_i$.

The plots *b*) of Figure 2, 3 and 4 show the predicted events (histogram) superimposed on the observed events, the background events b_i are also superimposed. In plots *c*) of Figure 2, 3 and 4 a pure exponential function with the fitted lifetime is superimposed on the background subtracted and $f(t')$ corrected t' distribution.

The measured lifetimes are: 408.75 ± 1.42 fs for $D^0 \to K^-\pi^+$, 411.25 ± 1.95 fs for $D^0 \to K^-\pi^+\pi^+\pi^-$ and 1039.42 ± 4.28 fs for $D^+ \to K^-\pi^+\pi^+$.

Our lifetime measurements have been tested by modifying each of the vertex and Čerenkov cuts individually. For example in Figure 5 one can see the measured lifetimes versus the ℓ/σ_ℓ detachment cut. The measured lifetimes of the three decay modes are stable with respect to ℓ/σ_ℓ. Our measured lifetimes show no significant variation with the cuts employed to extract the signal.

We check our D^0 lifetime evaluation partitioning the total sample into $D^\star-$tag and *no-tag* according to their origin. The obtained lifetimes are in very good agreement with the reported values.

To further check our lifetime measurements we have used tight cuts in order to extract a signal with virtually no background. Figure 6 shows the invariant mass plots of the three decay modes for this set of cuts. The lifetime measurements from these samples, 411.26 ± 3.11 fs for $D^0 \to K^-\pi^+$ 413.10 ± 4.80 fs for $D^0 \to K^-\pi^+\pi^+\pi^-$ and 1036.66 ± 8.00 fs for $D^+ \to K^-\pi^+\pi^+$, are in very good agreement with our previous determination.

Systematic uncertainties for these lifetime measurements can arise from several sources. We performed a detailed study to analyze these sources.

There is an uncertainty due to the absolute time scale which was determined by studying the absolute length and momentum scale in the experiment (see reference [9] for more details). We estimate an uncertainty of $\pm 0.11\%$ for this source.

Another source of systematic uncertainty is linked to the detector and reconstruction efficiency. The $f(t')$ corrects the reduced proper time distribution for these effects, but an uncertainty could originate if there is a mismatch between the Monte Carlo simulation and the data. We have verified that our Monte Carlo accurately reproduces several variables such as the longitudinal and transverse momenta, the multiplicity of the production vertex, the decay length and the proper time resolution. In order to estimate this uncertainty we split our total sample into independent subsamples depending on D momentum, particle versus anti-particle and the different periods in which the data were collected. The splits into D momentum and charge conjugation are the natural tests to reveal a possible mismatch between data and Monte Carlo because they probe the response of the detector. The main reason for the period dependence is the insertion of the upstream silicon system (which improved the resolution) in the target region during the 1997 fixed-target run period. A technique, employed in FOCUS and in the predecessor experiment E687, modeled after the *S-factor method* from the Particle Data Group [3], was used to try to separate true systematic variations from statistical fluctuations. The lifetime is evaluated for each of the 8 ($= 2^3$) statistically independent subsamples and a *scaled variance* is calculated; the *split sample* variance is defined as the difference between the reported statistical variance and the scaled variance if the scaled variance exceeds the statistical variance. This contribution to the systematic error is reported as *split sample* in Table 1.

The reported lifetimes are obtained with a particular set of fitting conditions. For example the width of the bins or the range of the t' distribution. This is a particular choice and the lifetime should be independent of it. We investigated if this could be a possible source of uncertainty by varying the width of the bins, the upper limit of the t' distribution, the location and the width of the sidebands, and the width of the signal region. In addition we studied the effect of using only the low or only the high mass sideband as well as the effect of elimininating the background term in the likelihood (the second term in equation 2). For all these *fit variants* the sample variance is used as an estimate of this uncertainty because the various measurements are all taken as *a priori* likely.

A further source of systematic error can be due to uncertainties in the target absorption corrections. Two effects are present: hadronic absorption of decay daughters which would increase the fitted lifetime if neglected and absorption of the D in the target which would tend to decrease the fitted lifetime if not taken into account. In our Monte Carlo all known particle absorption effects (values from Particle Data Group [3]) have been simulated for the decay daughters. For the charm hadron absorption our simulation assumes 1/2 of the cross section for neutrons. We estimate the uncertainty of this contribution by varying the charm cross-section by 50% and the daughter particle interaction cross-sections by 25% in the Monte Carlo simulation. We verify that these

Table 1
Contributions in percent to the systematic uncertainty.

Source	D^0 $K^-\pi^+$	D^0 $K^-\pi^+\pi^+\pi^-$	D^0 combined	D^+ $K^-\pi^+\pi^+$
Absolute time scale	0.11%	0.11%	0.11%	0.11%
Split sample	0.	0.37%	0.13%	0.
Fit variant	0.19%	0.14%	0.17%	0.15%
Absorption	0.11%	0.20%	0.20%	0.38%
Acceptance	0.21%	0.21%	0.21%	0.52%
Total systematic error	0.32%	0.50%	0.38%	0.67%

estimates, reported in Table 1, are consistent with a determination of this contribution obtained comparing the lifetimes of decays with the D produced in the upstream half of each target with those produced in the downstream half of the same target (see reference [10] for more details on the target setup). Each partition represents a different mixture of hadronic absorptions of decay daughters and D mesons.

The acceptance could be another source of uncertainty. We analyzed this effect determining the D^0 lifetime without the correction function $f(t')$ and removing the fiducial volume cut from the set of analysis cuts (this makes the correction function almost flat). We obtained results in good agreement with the reported values. This check is not possible for the D^+ because of the longer lifetime, a geometric acceptance correction is always needed. A study was performed in FOCUS (see reference [9] for more details) comparing the acceptance part of the Monte Carlo correction with the high statistics $K^0_S \to \pi^+\pi^-$ decays. The result of this study showed an excellent agreement between the acceptance observed in the data and the acceptance simulated by the Monte Carlo; however we assess a 2% uncertainty due to the finite statistics. This 2% uncertainty in the $f(t')$ correction function gives a 0.21% and 0.52% uncertainty in the lifetime of D^0 and D^+ respectively.

The finite Monte Carlo statistics give a negligible contribution to the systematic uncertainty.

Table 1 shows the contributions of each of these sources to the total systematic uncertainty. For the combined D^0 lifetime the systematic error (also shown in Table 1) is obtained combining the individual sources of systematic uncertainty from $D^0 \to K^-\pi^+$ and $D^0 \to K^-\pi^+\pi^-\pi^+$. We assume the absolute time scale and the absorption correlated. To obtain the final systematic error the uncertainties from the different sources are then added in quadrature.

The final lifetime values are 409.62 ± 1.15 (statistical) ± 1.55 (systematic) fs for

D^0 (weighted average) and 1039.42 ± 4.28 (statistical)± 6.97 (systematic) fs for D^+. A final check was performed for the D^0 lifetime. We compute the lifetime using a combined likelihood, that is forming a global likelihood for $K^-\pi^+$ and $K^-\pi^+\pi^-\pi^+$. The fit parameters are the two distinct backgrounds and one lifetime. The lifetime from the combined likelihood, 409.62 ± 1.15 (statistical), is identical to the reported value.

This measurement of the D^0 lifetime value is in very good agreement with the result we obtained in our lifetime difference paper[4].

In conclusion we have measured the lifetimes of the D^0 and D^+ mesons. Our results are reported in Table 2 along with a comparison with the most recent published measurements.

Table 2
Measured lifetimes ($\times 10^{-12}$ s).

Experiment	D^0	D^+
E687 [7]	$0.413 \pm 0.004 \pm 0.003$	$1.048 \pm 0.015 \pm 0.011$
CLEO II [11]	$0.4085 \pm 0.0041^{+0.0035}_{-0.0034}$	$1.0336 \pm 0.0221^{+0.0099}_{-0.0127}$
E791 [12]	$0.413 \pm 0.003 \pm 0.004$	
This measurement	$0.4096 \pm 0.0011 \pm 0.0015$	$1.0394 \pm 0.0043 \pm 0.0070$

Our results will significantly decrease the errors on the current world average values for the D^0 and D^+ lifetimes.

From our measurements of the D^0 and D^+ lifetimes we can update the determination of the ratio $\tau(D^+)/\tau(D^0)$: 2.538 ± 0.023. This result and the inclusive semileptonic branching ratios [3], $D^+ \to eX = (17.2 \pm 1.9)\%$ and $D^0 \to eX = (6.75 \pm 0.29)\%$, show that the D^0 and D^+ semileptonic decay widths are nearly equal:

$$\frac{\Gamma(D^0 \to eX)}{\Gamma(D^+ \to eX)} = \frac{B(D^0 \to eX)}{B(D^+ \to eX)} \times \frac{\tau(D^+)}{\tau(D^0)} = 1.00 \pm 0.12 \qquad (5)$$

This implies that differences in the total decay widths between D^0 and D^+ must be due to differences in the hadronic decay sector.

We wish to acknowledge the assistance of the staffs of Fermi National Accelerator Laboratory, the INFN of Italy, and the physics departments of the collaborating institutions. This research was supported in part by the U. S. National Science Foundation, the U. S. Department of Energy, the Italian Istituto Nazionale di Fisica Nucleare and Ministero dell'Università e della Ricerca

Scientifica e Tecnologica, the Brazilian Conselho Nacional de Desenvolvimento Científico e Tecnológico, CONACyT-México, the Korean Ministry of Education, and the Korea Research Foundation.

References

[1] See for example, I.I. Bigi, *Il Nuovo Cimento* **109 A** (1996) 713 and references therein.

[2] I.I. Bigi *et al.*, *Ann.Rev.Nucl.Part.Sci.* **47** (1997) 591.

[3] Particle Data Group, D.E. Groom *et al.*, *Eur. Phys. J.* **C15** (2000) 1.

[4] FOCUS Collaboration, J.M. Link *et al.*, *Phys. Lett.* **B485** (2000) 62.

[5] E687 Collaboration, P.L. Frabetti *et al.*, *Nucl. Instr. Meth.* **A320** (1992) 519.

[6] FOCUS Collaboration, J.M. Link *et al.*, hep-ex/0108011, to be published in *Nucl. Instrum. Methods* **A** .

[7] E687 Collaboration, P.L. Frabetti *et al.*, *Phys. Lett.* **B323** (1994) 459.

[8] T. Sjostrand, *Computer Physics Commun.* **82** (1994) 74.

[9] FOCUS Collaboration, J.M. Link *et al.*, hep-ex/0202001, to be published in *Phys. Rev. Lett.*.

[10] FOCUS Collaboration, D. Pedrini *et al.*, *Nucl. Phys. Proc. Suppl.* **75B** (1999) 105.

[11] CLEO Collaboration, G.Bonvicini *et al.*, *Phys. Rev. Lett.* **82** (1999) 4586.

[12] E791 Collaboration, E.M. Aitala *et al.*, *Phys. Rev. Lett.* **83** (1999) 32.

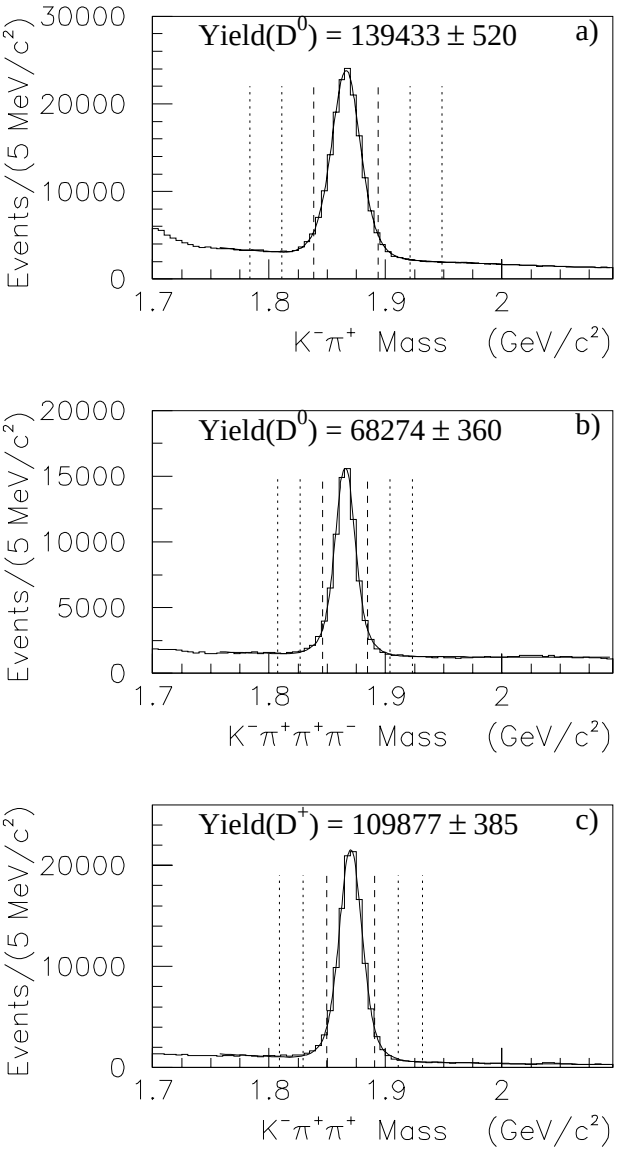

Fig. 1. (a) $K^-\pi^+$ invariant mass distribution, (b) $K^-\pi^+\pi^+\pi^-$ invariant mass distribution, (c) $K^-\pi^+\pi^+$ invariant mass distribution. The fits (solid curves) are described in the text and the numbers quoted are the yields. The vertical dashed lines indicate the signal region, the vertical dotted lines the sideband.

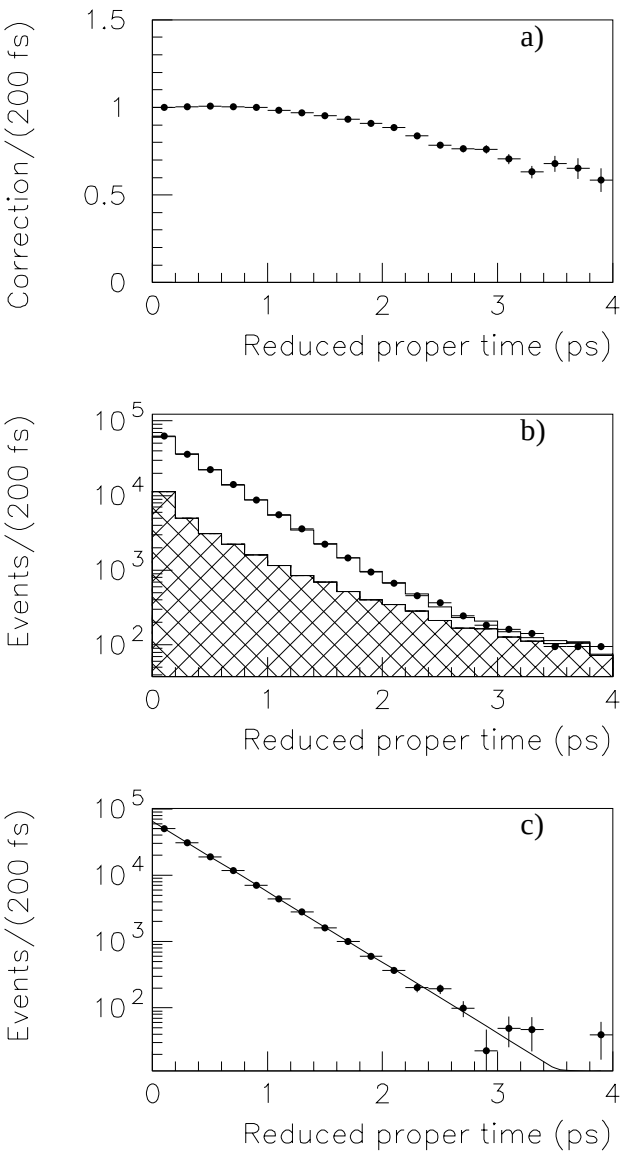

Fig. 2. Decay mode $D^0 \to K^-\pi^+$: (a) the correction function $f(t')$, deviation from a flat distribution represents the correction from a pure exponential function; (b) the predicted events (histogram) are superimposed to the observed events (points), the shaded distribution shows the t' distribution of the background; (c) the background subtracted and $f(t')$ corrected t' distribution, the superimposed straight line is an exponential with the fitted lifetime.

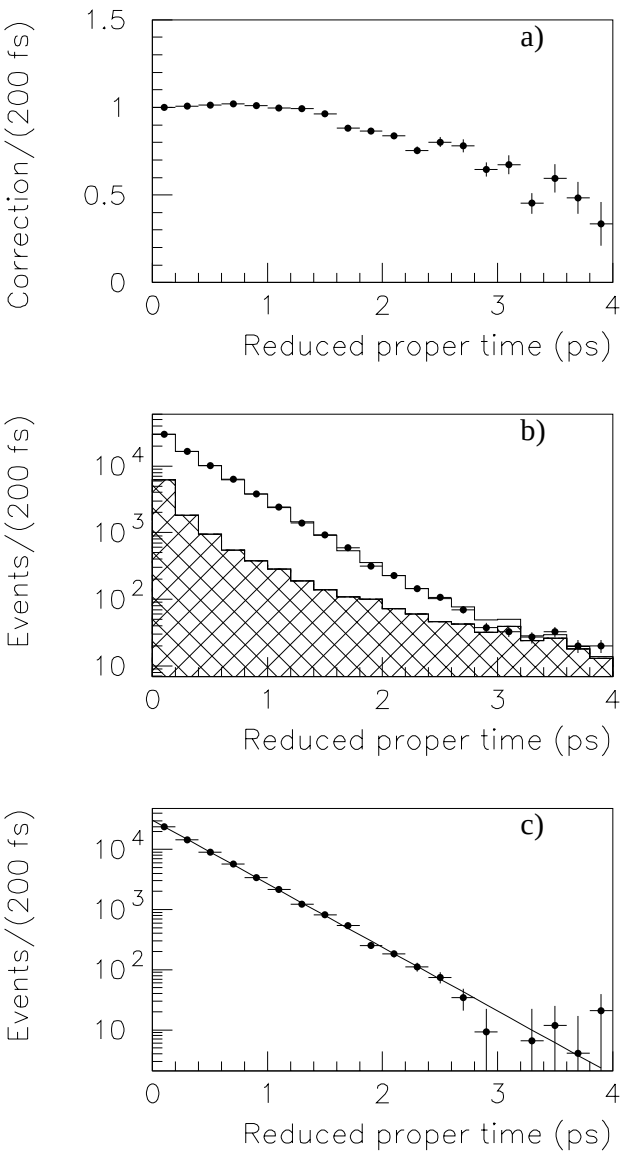

Fig. 3. Decay mode $D^0 \to K^-\pi^+\pi^-\pi^+$: (a) the correction function $f(t')$, deviation from a flat distribution represents the correction from a pure exponential function; (b) the predicted events (histogram) are superimposed to the observed events (points), the shaded distribution shows the t' distribution of the background; (c) the background subtracted and $f(t')$ corrected t' distribution, the superimposed straight line is an exponential with the fitted lifetime.

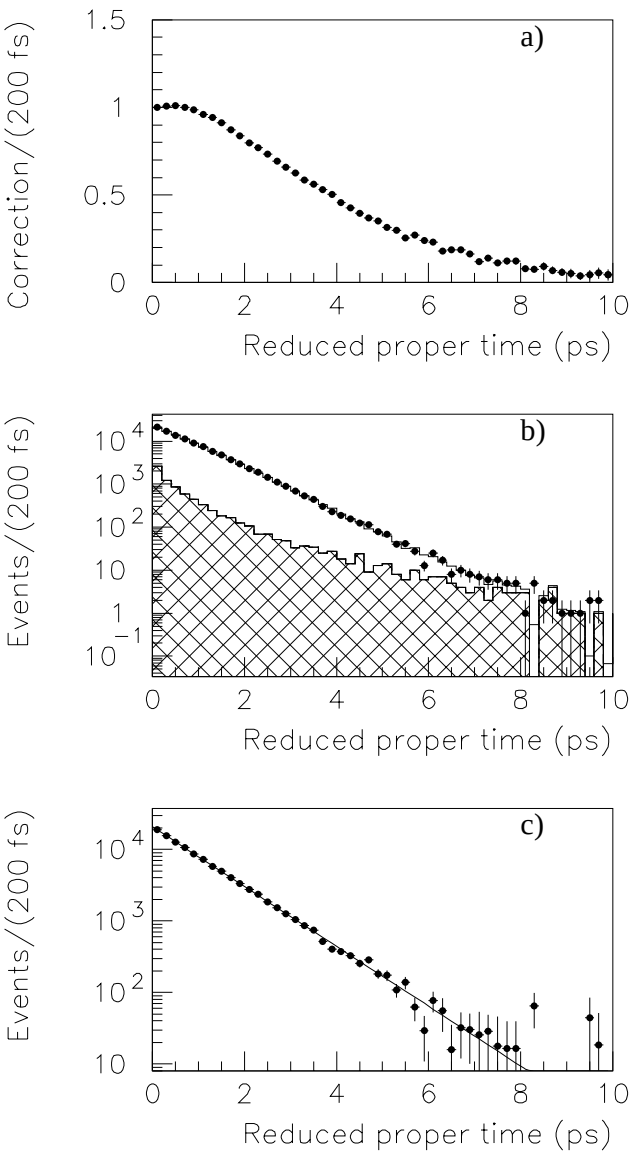

Fig. 4. Decay mode $D^+ \to K^-\pi^+\pi^+$: (a) the correction function $f(t')$, deviation from a flat distribution represents the correction from a pure exponential function; (b) the predicted events (histogram) are superimposed to the observed events (points), the shaded distribution shows the t' distribution of the background; (c) the background subtracted and $f(t')$ corrected t' distribution, the superimposed straight line is an exponential with the fitted lifetime.

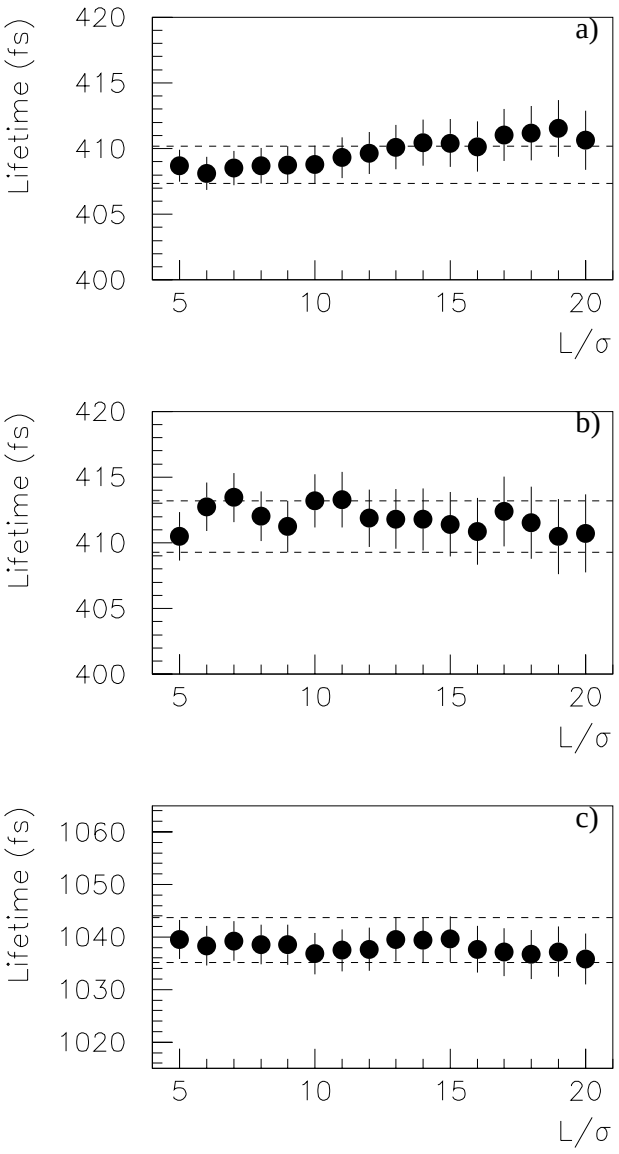

Fig. 5. The fitted lifetime versus the ℓ/σ_ℓ detachment cut for: (a) $D^0 \to K^-\pi^+$, (b) $D^0 \to K^-\pi^+\pi^+\pi^-$ and (c) $D^+ \to K^-\pi^+\pi^+$. The horizontal dashed lines show the interval corresponding to the chosen lifetime $\pm 1\sigma$.

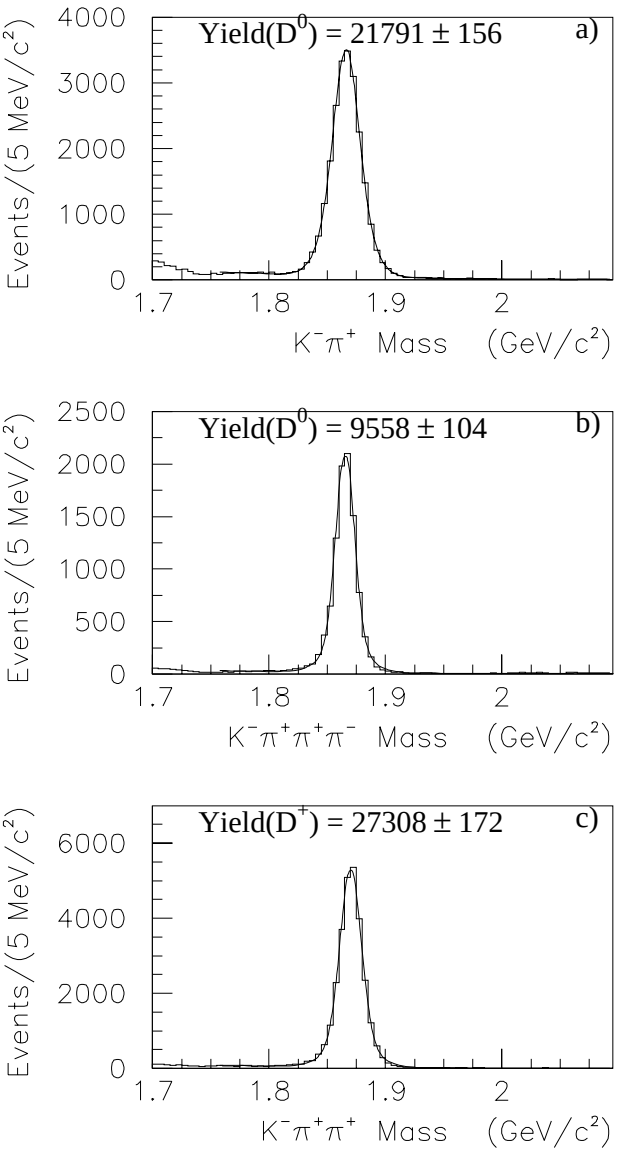

Fig. 6. Invariant mass distributions obtained using tight cuts for: (a) $K^-\pi^+$, (b) $K^-\pi^+\pi^+\pi^-$ and (c) $K^-\pi^+\pi^+$. The functions used to fit the data (solid curves) are similar to those of Figure 1 and the numbers quoted are the yields.